Parametric study of reactivity changes in Egypt second research reactor (ETRR-2)

Mohamed E. Nagy [a], Mohamed M. Elafify [a] and Ashraf M.R. Enany [b]
[a] *Nuclear Eng. Department, Faculty of Engineering, Alexandria University, Alexandria, Egypt*
[b] *Atomic Energy Authority, INSHAS, ETRR-2, P.O.Box 13759, Cairo, Egypt*

The reactivity parameter is one of the important neutronic parameters that must be studied for the reactor safety evaluation as well as for the reactor operation follow-up. Reactivity is an integral parameter normally used to describe the overall state of a nuclear reactor. A numerical study of the important parameters that change the reactivity in ETRR-2 is presented in this paper. The study is carried out through the comparison between the measured and the calculated values of these parameters for several different assembled cores. The values include the reactivity calculational error of criticality determination, control plate worths, reactivity excesses, shutdown margins and the calculated Xenon equilibrium levels at different reactor powers. The calculated values of all the above parameters are very close to the measured ones. This means that the adopted calculational models and their associated neutronic libraries are capable of representing ETRR-2 core.

يتناول هذا البحث إجـراء الحسابـات النيترونية المختلفة للعديد من المعاملات المؤثرة بشكل كبير على تعيـين مفاعليـة قلـب المفاعل وذلك للتحـقق والتأكد من مدى صحة ودرجة كفاءة الإجراءات الحسابية المستخدمـة. وقـد تمـت مقـارنـة القـيم المحسوبة لهذه المعاملات النيترونيـة بنظيراتها المقاسة خـلال مرحلة التدشـين لحالات أوضـاع تـشغيل مختلفـة لقلـب المفاعل. لقد أوضحت المقارنة بين قيم النتائج المحسوبة وتلك المقاسة لهذه المعاملات مثل كفـاءة قـضبان الـتحكم، والفاعليـة المزادة، وأوضاع قضبان التحكم لتحديد الحالات الحرجة، ومفاعلية مادة الكوبلت بقلب المفاعـل ومـستويات التـشبع لعنـصر الزينون عند قدرات تشغيل مختلفة وغير ذلك من المعاملات الأخرى، أوضحت أن هناك تقارب كبير بـين القـيم المحـسوبة والمقاسة. يعزى هذا التقارب إلى دقة بيانات المقاطع العرضية المحسوبة للمواد المختلفة وأيضا إلـى التمثيـل الجيـد للنمـاذج الحسابية المطبقة فى حساب المعاملات النيترونية.

Keywords: Reactivity, Neutronic calculations, Control plate worth, Criticality, Core configurations

1. Introduction

The neutronic calculations of the research reactors, especially those pertained to the Material Test Reactors (MTRs), have recently received great attention in the published literatures all over the world. This is because of the implementation of the international Uranium Enrichment Reduction Program (UERP) [1]. As a result, the well-developed neutronic calculational codes for the power reactors are modified, adopted and used to MTRs. An extensive review of the relevant publications shows that the worldwide MTRs core neutronic calculations follow almost two directions, the first is to use the Diffusion approximation approach and the second is to use the monte carlo approach.

Diffusion Approximation Approach: The philosophy of the calculational procedure in this approach is to start with small systems, like a fuel plate cell, and to proceed via intermediate systems, like a fuel assembly, and moves towards the entire reactor core. Hence, the approach is mainly divided into two steps:

a) Cell calculation: It is used to calculate macroscopic cross sections of different materials for the core calculation.

b) Core calculation: It is used to calculate neutronic parameters of the core such as neutron fluxes, power and burn-up distribution, reactivities, cycle length, kinetic parameters, etc.

It can be noticed through the following relevant review that different versions of the cell calculations code WIMS is used almost all over the world, while different codes of diffusion exist for the global core calculations. S.I. Bhuiyan et al. [2], have made neutronic feasibility studies of the 3 MW TRIGA MARK II research reactor in Bangladesh for upgrading.

The overall strategy they followed is: (i) generation of problem dependent cross section library from basic Evaluated Nuclear Data Files (ENDF) such as ENDF/B-VI [3], (ii) use WIMS code to generate cell constants for all of the materials in the core and its immediate neighborhood, (iii) use CITATION 3 to perform 3-D global analysis of the core to study multiplication factor, neutron flux and power distribution, power peaking factors, temperature reactivity coefficients, etc., (iv) check the validity of the deterministic codes with the Monte Carlo code MCNP4B and (v) reshuffle the current core configuration to achieve the desired objectives. W. L. Woodruff et al. [4] have used the supper cell option in WIMSD-4M to treat non-lattice geometry. This capability provides properly homogenized and resonance corrected fuel regions, improved spectra for non-fuel regions and proper treatment for regions containing experimental fuel or other resonance materials. This option was applied to several diverse geometries and compared with VIM Monte Carlo data [4]. The methods and codes used for neutronic calculations of the Maria research reactor were presented by K. Andrzejewski et al. [5]. They have used the two versions of the WIMS code namely WIMSD-5 and WIMS-ANL as a cell code. For global reactor calculation they used the 3D transport code TRITAC and compared the results with the MCNP code.

Monte carlo approach: This approach consists of a combination of Monte Carlo and burn-up codes alternatively. The following relevant review illustrates how this approach is applied. In the last few years, the Monte Carlo Neutron and Photon transport code (MCNP) has been used extensively in the Reduced Enrichment for Research and Test Reactors (RERTR) program at Argonne National Laboratory and the EREBUS code is used for the burn-up analysis. Nabbi et al. [6] have used a sophisticated method for FRJ-2 research reactor. In their calculations they coupled the MCNP code with a depletion code. In each time step, representing a time interval in the operation history fuel burn-up is determined on the basis of neutron cross sections and local fluxes from the previous step of the MCNP run. Yoshihiro NAKANO et al. [7] have performed the neutronics characteristics tests of the JRR-4 LEU core. They used the continuous energy Monte-Carlo code MVP which can handle complicated structures with minimum geometrical approximations. History of 600,000 is selected to have one standard deviation error of about 0.1 % $\Delta k/k$. G. Hordsy et al. [8] have used the MCNP4A code to calculate the upgraded VVR-SM type (Russian design) Budapest Research Reactor using 36% enriched uranium.

In ETRR-2, well-known and validated neutronic calculational cell and core codes are linked together in a computational package called "MTR_PC system" to constitute the adopted ETRR-2 calculational line that is followed to carry out the required neutronic calculations for safety evaluation and follow-up operation. All the used codes belong to the MTR_PC calculational system and they are:

I) The nuclear data library used for calculation is the original WIMS-D4 library with updates from ENDF/B-IV of Ag, In, Cd, and Gd. [9]

II) WIMS-D4 [10]. The collision probabilities option in one dimensional geometry (slab) is used for cell calculation.

III) POS_WIMS [11]. This program is used to homogenize and condense macroscopic cross sections from WIMS calculation.

IV) CITVAP 3.1 [12]. It is a core diffusion code. It is a new version of CITATION II program.

V) HXS 4.1 [13]. It is the macroscopic cross section library manager program. It is used for the interface between cell and core calculation.

1.1. Application to ETRR-2

The set of codes that have been mentioned are used to study the parameters that affect reactivity in ETRR-2 as an example of the model. Five different core configurations were analyzed in depth, namely water reflected, with Beryllium reflectors (1 and 2 faces reflected) and with and without the in-core cobalt irradiation device. One important feature of the core configuration is that there are three types of Fuel Elements (FEs) which have the same enrichment value but with different ^{235}U mass content namely, type-1, type-2 and standard-type. The following sections briefly describe the core characteristics of the ETRR-2 reactor, the calculation

codes and models, a detailed comparison between calculations and measurements that were carried out.

1.2. ETRR-2 core description

The ETRR-2 core is an array of fuel elements, reflectors, absorber plates, gadolinium injection boxes and irradiation devices. The basic geometric unit in the x-y core array is a square shape of 8.1 x 8.1 cm^2. It can be used for fixing a fuel element, an irradiation device or an empty box.

There is a 30-position grid with a 6x5 configuration inside the chimney as shown in fig. 1. It is divided by two structural guide plates (for control plates insertion). The reactor uses MTR fuel type of a square section of (8 x 8) cm. Each fuel element has 19 fuel plates separated from each other by a 0.27 cm coolant channel. The fuel plate meat is made of U_3O_8 with an enrichment of 19.75 ^{w} % ^{235}U. The active zone of fuel plate dimensions is 80 cm length, 6.4 cm width and 0.07 cm thickness. The reactor control is accomplished through 6 independent Ag-In-Cd alloy-absorbing plates claded with stainless steel. Each absorbing plate moves vertically inside a fixed guide box located parallel to the chimney. Around the chimney there is an external grid array. The irradiation grid has locations where reflectors, empty boxes and irradiation devices can be placed.

2. Investigated core configurations

Five different core configurations were assembled during the low power test of the commissioning; the core configurations measured were:

I) Core SU-29 (Start Up Core with 29 FEs). It was the first measured core configuration. It has 29 fuel elements and no Beryllium reflectors as shown in fig. 1.

II) SU-29-1Be. The Beryllium reflectors were added sequentially from core SU-29, starting with the core SU-29-1Be (only one core face with Beryllium reflectors, row C in the irradiation grid).

III) Core SU-29-2S differs from the 1/98 in one Beryllium reflector in position C-10 and the irradiation boxes.

IV) Core 1/98 (The first digit is a correlative number and the last two digits are the year, then 1/98 is the first core in 1998), it is shown in fig. 2.

V) Core 2/98. It has the same configuration as in Core 1/98 but with the Cobalt irradiation device inside the in-core Cobalt irradiation position (position D3).

2.1. Calculational models

For the evaluation of the cell constants the WIMS code is used in slab geometry. The core calculation is performed with the CITVAP diffusion code in x-y-z with an energy discretization of three groups as: Group1: (10 to 0.821) MeV ,Group2: (0.821 MeV to 0.625 eV) and Group3: (0.625 to 0.0) eV. A conceptual description of the computational models of the most important core components is given in the following:

2.1.1. Fuel element zone

One homogenous zone model of the fuel element is adopted for the neutronic calculations of the ETRR-2 core. A verification of that model adequacy to represent the fuel element is presented in another paper by the same authors. The fuel cell calculation is performed with an energy discretization of 12 groups (partitions 5, 15, 20, 23, 25, 27, 30, 34, 45, 51, 57 and 69 in the 69 group structure). The cell constants are evaluated versus the burn-up values at steps from 0 to 120000 MWD/T (~70% ^{235}U atom consumption). For core calculations, the cross sections are homogenized and condensed from 12 to 3 groups as presented above. The dimensions of the reactor core zone (*x, y, z*) for modeling are 120 x 97 x"20+ 80+20" cm (80 cm is the active length of the fuel element in z-direction and two equal water layers are added axially, one of them at 20 cm above and the other is under the active length of the fuel elements). The active length of the fuel element is divided into 20 axial segments of 4 cm each.

2.2.2. Control element zone

The irregular shape of the guide plate boxes and the change of the material filling the control plate area due to the control plate movement during reactor operation requires

the division of the whole control plate zone into different sub-zones for cell and core calculations. These sub-zones are:

I) A zone of Aluminum and water outside the active width of the absorber, corresponding with the ends of the guide box.

II) If the absorber plate is in, there is a homogenized zone of Aluminum, water, stainless steel, Helium and Ag-In-Cd.

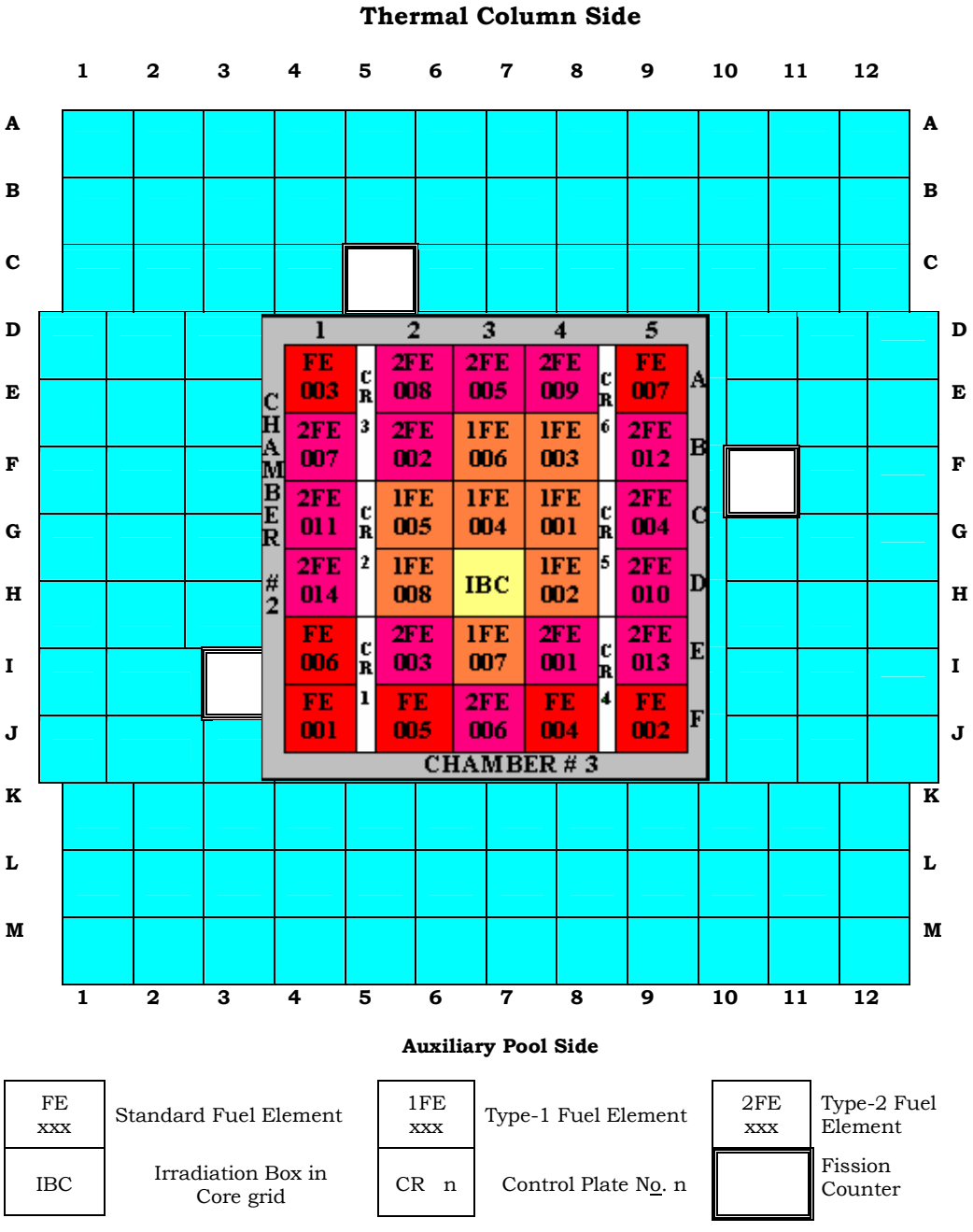

Fig. 1. Core configuration for the core SU-29.

III) If the absorber plate is out, the space it leaves in the guide box is occupied with the follower rod (coupling rod). The model has two homogeneous regions:

a) The region outside the follower: Aluminum and water.
b) The follower region: Aluminum, water and stainless steel.

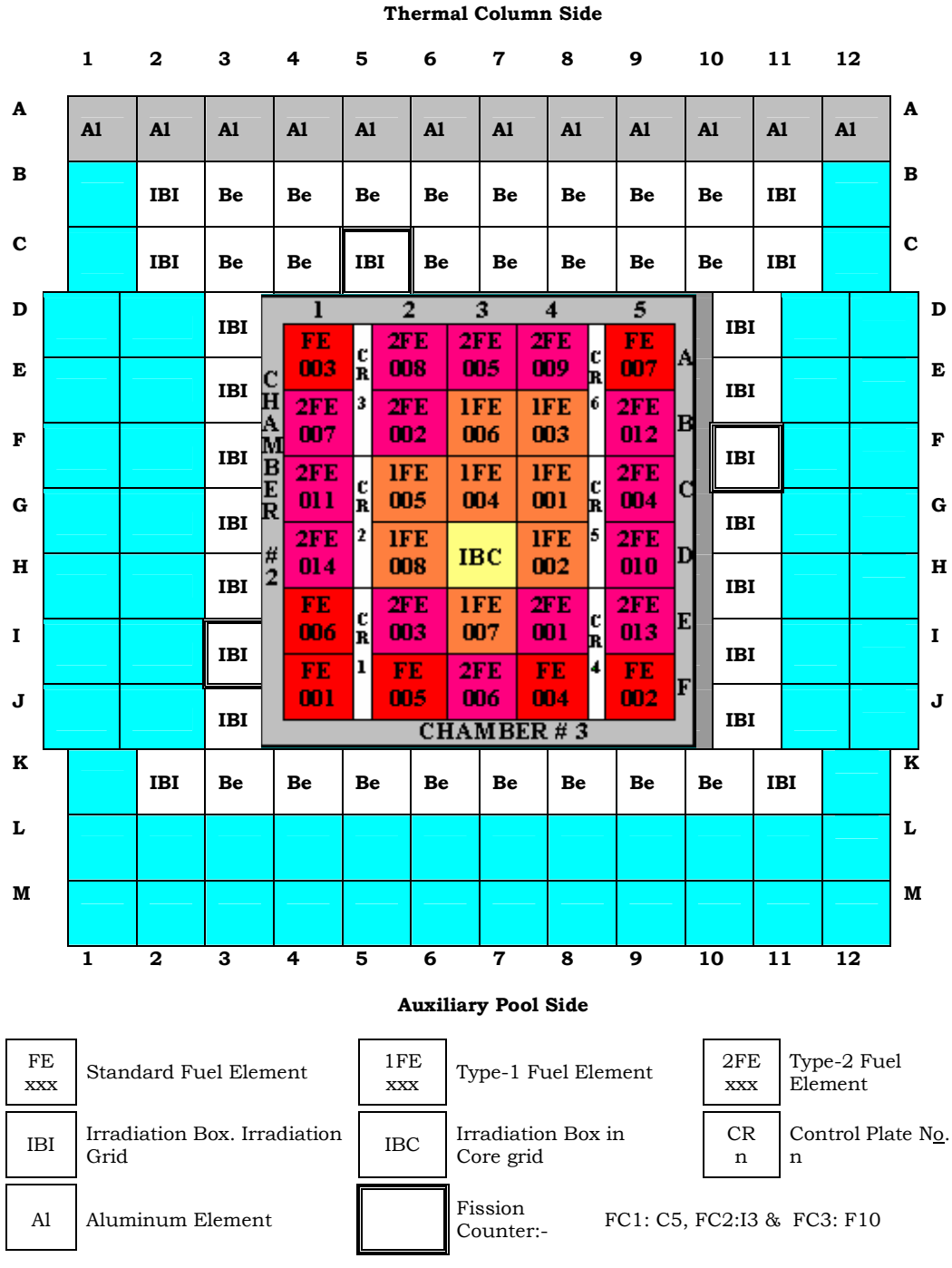

Fig. 2. Core configuration for the core 1/98.

Table 1
Critical states of core SU-29

Case No.	Control plate positions (% Extraction)						Reactivity (pcm)
	CR-1	CR-2	CR-3	CR-4	CR-5	CR-6	
01	100	100	100	100	41.5	100	229
02	83.3				46.0		218
03	75.0				50.0		205
04	66.8				54.5		190
05	61.1				58.0		179
06	57.0				63.0		211
07	52.0				67.8		209
08	46.6				72.2		182
09	42.2				76.7		174
10	36.0				83.0		204
11	29.7				90.5		200
12	24.1				100		219
Average calculated reactivity							202
Standard deviation							17
13	100	100	100	100	50.5	60.0	195
14					54.2	52.4	176
15					59.7	44.9	223
16					63.9	37.5	179
17					69.2	30.7	214
18					73.7	28.0	224
Average calculated reactivity							201
standard deviation							22

2.2.3. Chimney zone (gadolinium injection zone)

The gadolinium injection zone is divided into different zones at core level calculation:
a) The corner of the chimney: which is made of pure Zircalloy.
b) The horizontal faces (see figure 1) of the chimney have different water gaps from the vertical ones. This is approximated by averaging the water gaps.

3. Parametric study

3.1. Reactivity error of criticality in the developed model

The calibration process of a control plate requires criticality of the reactor with a proper control plate pattern at a very low power (without feedback effects), without external neutron sources or neutron poisons changing with time. Then the critical pattern is changed slightly by moving the control plate under calibration named (A) to put the reactor supercritical for a while. After that, the reactor is put critical again with a slightly different pattern from the previous critical one by moving another control plate named (B) in the opposite direction of (A). Therefore, during the calibration process of the control plates, many different critical cores were obtained and the control plate positions were recorded for each critical case. The recorded positions of the control plates are used as input data in the core calculation code (CITVAP) and the reactivity value of the core is calculated to obtain the calculational error for each critical case. The used reactivity unit used is pcm unit where,

$$1\ pcm = 0.00001\,\frac{\Delta k}{k}.$$

An example of reaching criticality with different combinations of two control plates is

shown in table 1. The table shows 12 critical patterns with control plates number 1 and 5. The other 6 critical patterns are given at the end of the table for control plates number 5 and 6.

Table 2 shows many different critical core cases reached mainly during control plate calibrations for different core configurations. It is worth mentioning that the calibration process may be carried out with two or three different control plate combinations for the same core configuration.

The values in the table show that the reactivity calculational error of criticality determination is not the same for all cases, so it is necessary to determine the corresponding error for each configuration. The errors in calculated reactivity values are acceptable from the operational point of view which means that the model of calculations is reliable.

3.2. control plate worths

According to the operating regulations of the ETRR-2, two control plates must be specified as safety and the other four as control (regulating) plates [14]. The regulating plates control the excess reactivity, compensate the build-up of poisons and the fuel burn-up and are also used to put the reactor critical at different power levels. The positive period method [15] of control plate calibration is utilized to determine experimentally the control plate worth. Therefore, the reactor is made supercritical by withdrawing the control plate under calibration to a certain amount (~ 5 cm), and the resulting (positive) period is determined from the measured doubling time to derive the change in reactivity.

For every core configuration some control plates were calibrated to know the excess reactivity of the core. Not all plates were calibrated but some of them were compensated against a previously calibrated control plate. In any case, the effective delayed neutron fraction used to compare measured and calculated data was taken as β_{eff} = 750 pcm.

3.2.1. Core SU-29

The control plate number 5 (CR-5) was calibrated against CR-1. Table 3 shows the calculated and the experimental worth values of the control plates as well as their initial critical extraction percentage between square brackets.

Fig. 3 shows the comparison between calculated and measured values of control plate worth in dollar ($). The calculated values are always higher than the experimental ones. The difference between the two is in the range of 0.05 to 0.14 $, but both show the same behavior. The difference is due to the calculational process and inaccuracy in measurements.

Table 2
The critical cases of different core configurations

Core configuration	# of Combinations	# of Critical cases	Average calculated reactivity (pcm)	St. deviation (pcm)
SU-29	2	12 & 6	202 , 201	17, 22
SU-29-1Be	2	13 & 6	233 , 245	21, 12
1/98	3	19, 4 & 4	255 , 239 , 254	18, 8, 16
2/98	3	21, 5 & 4	269, 198 , 240	11, 21, 13
Total number of critical Cases = 94				

Table 3
Data of control plate calibration of core SU-29

Initial critical pattern: [100, 100, 100, 100, 41.5, 100]				
			Control plate worth (W) $	
Pattern	CR-A [range]	CR-B [range]	Measured [W_m]	Calculated [W_c] & [($W_c \div W_m$)-1] %
No. 1	CR-1 [100 – 24.1]	CR-5 [41.5 - 100]	2.14	2.22 [+4]

3.2.2. Core SU-29-2S

CR-5 was calibrated against CR-3 and CR-6. CR-1 was compensated with CR-5 and CR-3. Table 4 shows the calculated and the experimental values of the control plate worths as well as the initial critical position of different control plate combinations. Figs. 4 and 5 are the graphs of the calculated and the experimental values of CR-5 and CR-1.

Fig. 4 clearly shows the common S-shape behavior of reactivity worth and control plate extraction for both calculated and experimental values. The calculated values are always higher than the experimental ones where the difference between the total measured and calculated worth is not greater than 2%. Fig. 5 shows that the experimental compensation is applied to obtain the worth of CR-1. It must be taken into account that in compensations the experimental values are masked by control plate shadowing effects. The experimental values are higher and the difference between the total measured and calculated worth is not more than 3%.

3.2.3. Core 1/98

CR-1 was calibrated against CR-4. CR-2 was compensated with CR-4 and CR-6 was compensated also with CR-4. Table 5 shows the calculated and the measured values. Figs. 6, 7 and 8 are the graphs of the calibrated CR-1, 2 and 6.

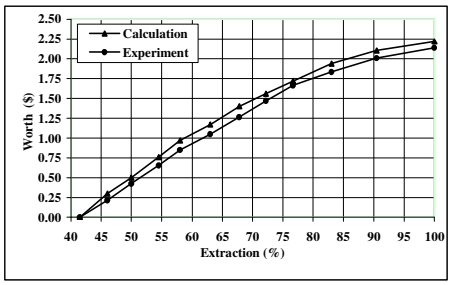

Fig. 3. Experimental Calibration of CR-5 of core SU-29.

Table 4
Data of control plate calibration core-29-2S

Initial critical pattern (No. 1): [0, 100, 79.1, 100, 0, 100] Initial critical pattern (No. 2): [0, 100, 49.4, 100, 100, 0]				
			Control plate worth (W) $	
Pattern	CR-A [range]	CR-B [range]	Measured [W_m]	Calculated [W_c] & [$(W_c \div W_m)$-1] %
No. 1	CR-3 [79.1 - 0] & CR-6 [100 -45.0]	CR-5 [0 - 100]	3.97	4.03 [+2]
No. 2	CR-5 [100 – 0.0] & CR-3 [35.0 - 0.0]	CR-1 [0 - 100]	5.57	5.38 [-3]

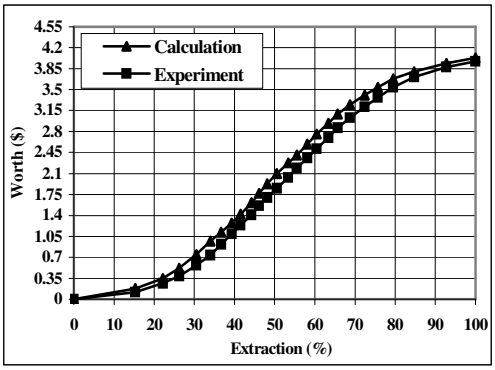

Fig. 4. Experimental calibration of CR-5 of core SU-29-2S.

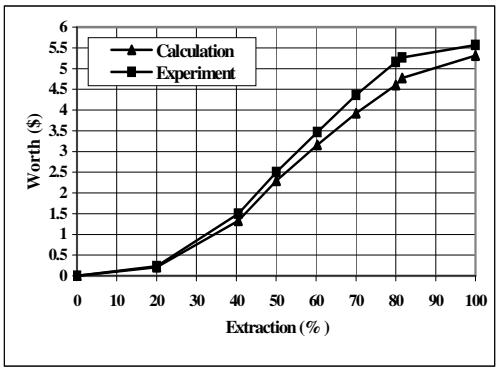

Fig. 5. Experimental compensation of CR-1 of core SU-29-2S.

Table 5
Data of control plate calibration of core 1/98

Initial critical pattern (No. 1): [0, 53.5, 100, 100, 100, 0] Initial critical pattern (No. 2): [0, 52.8, 100, 100, 100, 0] Initial critical pattern (No. 3): [0, 52.8, 100, 100, 100, 0]				
Pattern	CR-A [range]	CR-B [range]	Control plate worth (W) $	
			Measured [W_m]	Calculated [W_c] & [($W_c \div W_m$)-1] %
No. 1	CR-4 [100 – 0.0] & CR-2 [53.5 – 52.4]	CR-1 [0 – 100]	3.66	3.75 [+2]
No. 2	CR-4 [100 – 54.0]	CR-2 [52.8 - 100]	1.63	1.66[+2]
No. 3	CR-4 [100 - 0] & CR-2[52.8 – 49.7]	CR-6 [0 – 100]	3.82	3.5 [-8]

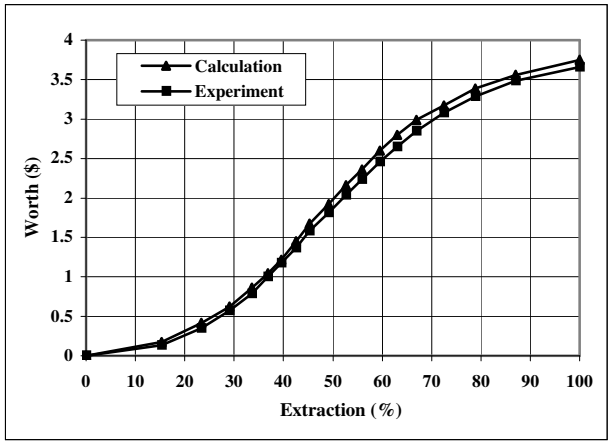

Fig. 6. Experimental calibration of CR-1 of core 1/98.

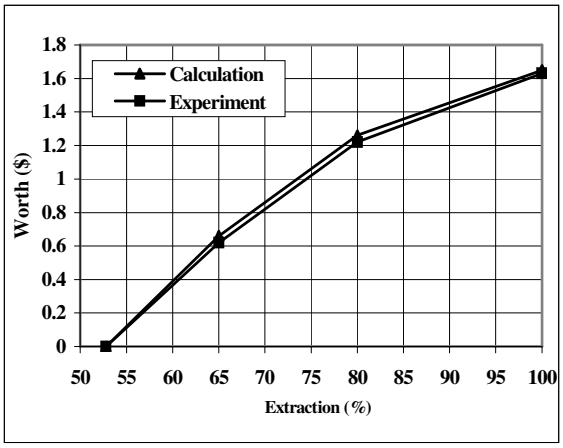

Fig. 7. Compensated calibration of CR-2 of core 1/98.

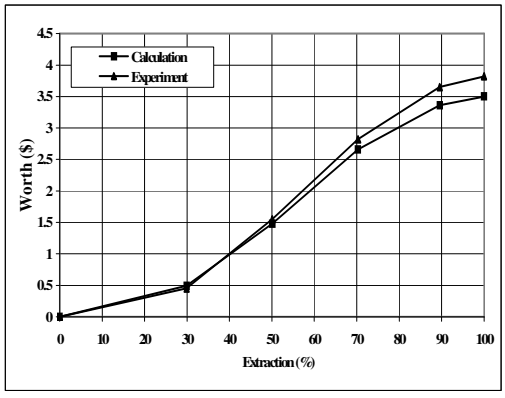

Fig. 8. Experimental compensation of CR-6 of core 1/98.

Fig. 6 shows that the calculated and the measured values of CR-1 have the same profile and indicates the common S-shape. The difference between the total measured and calculated worth is about 2%. Fig. 7 shows the experimental compensation of CR-2 with a difference between the total measured and calculated worth of about 2%. Fig. 8 shows the experimental compensation of CR-6 with a relatively large difference between the total measured and calculated worth due to the shadowing effect between the two compensating control plates

3.2.4. Core 2/98

CR-1 was calibrated against CR-4 and CR-2. CR-6 was compensated with CR-1. Table 6 shows the calculated and the experimental values of the control plate worths as well as the initial critical position of control plates for each calibration process. Figs. 8 and 9 are the graphs of the calibrated CR-1 and CR-6.

Fig. 9 shows that the calculated and the experimental values have the same behavior and the error between both total worth values is less than 1%. Fig. 10 shows the experimental compensation of CR-6 with a relatively large difference between the total measured and calculated worth due to the shadowing effect between the two compensating control plates.

3.3. Excess of reactivity and shut down margin

The excess reactivity was measured by the calibration and compensation method. Table 7 shows the measured and calculated excess of reactivity and shut down margin of different core configurations.

3.4. Xenon equilibrium levels

Xenon (^{135}Xe) is produced directly from fission and from the Beta decay of ^{135}I (in view of the fact that ^{135}Tl decays so rapidly to ^{135}I), as shown below.

^{135}Te ($t_{1/2}$ =11sec)→ ^{135}I (6.7 hr)→^{135}Xe (9.2 hr)
↑(fission) ↑(fission)
→ ^{135}Cs(2.3x10^6 yr) → ^{135}Ba

Because the half life ($t_{1/2}$) of ^{135}I and ^{135}Xe is so short and the absorption cross section of ^{135}Xe is so large, the concentration of these isotopes quickly raise to their equilibrium values. The xenon concentration can be calculated by WIMS code only at the equilibrium level. Fig. 11 shows the negative reactivity due to the maximum xenon concentrations at different power levels. Fig. 12 shows the rate of change of the reactivity with the power due to the maximum Xenon concentrations at different reactor powers. For the reactor powers below 6 MW, it was noticed that a small variation in the power leads to a large variation in the Xenon equilibrium level.

Table 6
data of control plate calibration of 2/98 core

Initial critical pattern (No. 1): [0,100,100,100,100,21.1] Initial critical pattern (No. 2): [100,75,100,0,100,21.1]				
			Control plate worth $	
Pattern	CR-A [range]	CR-B [range]	Measured [W_m]	Calculated [W_c] & [($W_c \div W_m$)-1] %
No. 1	CR-4 [100 - 0] & CR-2 [100 – 76.8]	CR-1 [0 – 100]	3.85	3.89 [+1]
No. 2	CR-4 [100 – 24.1]	CR-6 [21.1-100]	3.37	3.18 [-6]

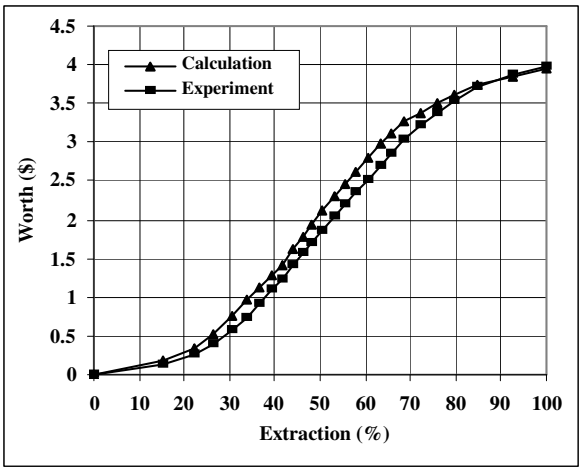

Fig. 9. Experimental calibration of CR-1 of core 2/98.

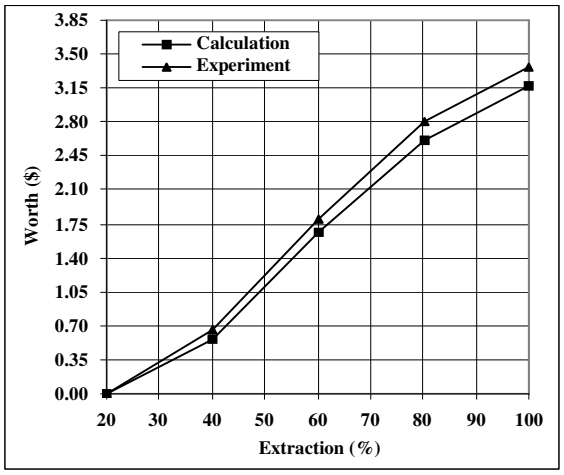

Fig. 10. Experimental compensation of CR-6 of core 2/98.

However, for the reactor powers above ~ 6 MW, the variation of Xenon equilibrium level with reactor power becomes less up to about 20 MW where the maximum reactivity becomes considerably constant (~3600 pcm = 4.8 $)

4. Fuel burn-up distribution at the end of core 2/98 operation

Each fuel element is divided into 20 axial segments of 4 cm each where the burn-up value of each segment is calculated. The main features of the reactor operation in the low power test period during the commissioning program are:
- Operation with large number of different critical control plate patterns
- Operation at different power values and relatively short and unequal time of operating intervals

Fig. 13 shows the average calculated burn-up distribution (MWD/T) of each fuel element at the end of the operation of core 2/98. The total burn-up value of this core is 187 MWD/T which is equivalent to 0.298 Full Power Days (FPDs) or to a decrease of 55 pcm in the core excess reactivity.

The fuel burn-up during the previous operating periods was insufficient to judge the effect of this parameter on the core reactivity. To study this parameter, further calculations had to be done on the core after a long time of reactor operation.

5. Conclusions

The analysis of the obtained measured and calculated results of different core parameters given in the previous tables and figures during the low power test period shows that:
I) For reactivity calculational error of criticality determination, it is necessary to determine the corresponding error for each configuration where the error is not the same for all cases. However, there is a very good agreement between the experimental values and the related calculated ones for all core configurations. From the operational point of view, the calculations for the determination of the criticality are reasonably accurate and well accepted.

Table 7
Excess of reactivity and shut down margin

Core	Excess of reactivity ($)		Shut down margin ($)	
	Measured	Calculation	Calculation	Measured
SU-29	2.14	2.22	19.3	19.9
SU-29-2S	10.19	9.95	13.11	12.8
1/98	9.11	8.91	12.7	13.9
2/98	7.22	7.07	17.1	18.4
CID* Worth	1.57	1.67		

* CID: cobalt irradiation device.

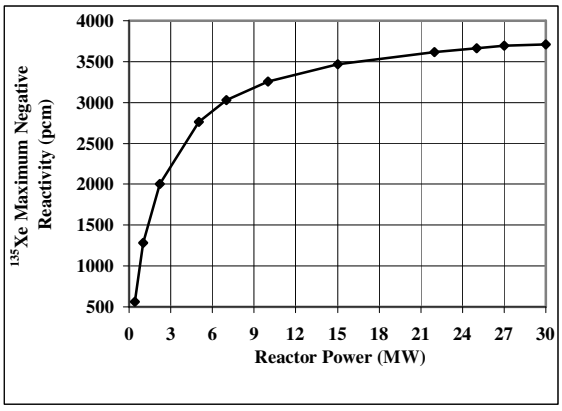

Fig. 11. The relation between ^{135}Xe negative reactivity and the power levels.

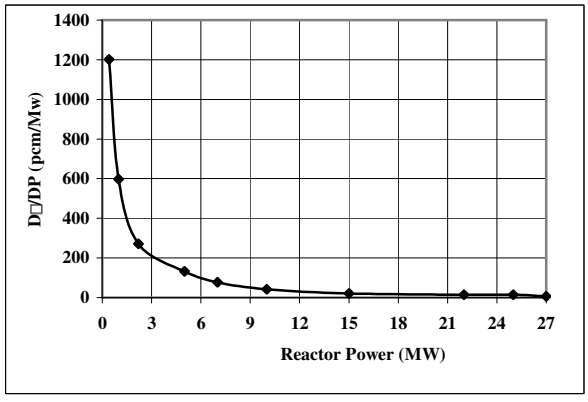

Fig. 12. The rate change of reactivity with the reactor power levels.

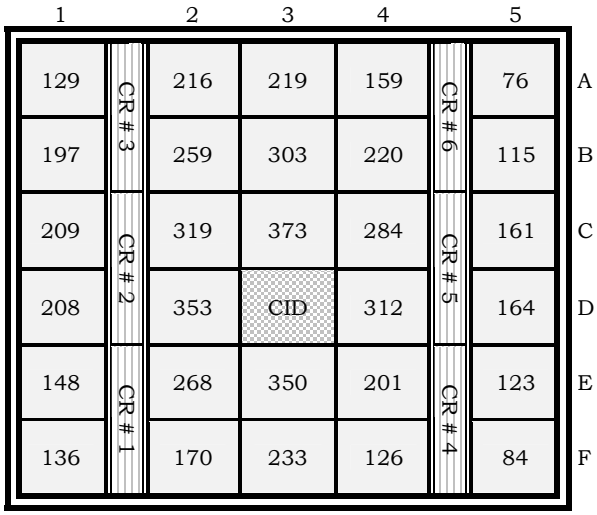

Fig. 13. Average burn-up distribution of the core 2/98 in MWD/T.

II) The calculation value of the excess reactivity of each core configuration is very close to the related measured one and is accurate enough to obtain other concerned operating parameters such as the cycle length, the reactivities at the beginning and at the end of cycle, shutdown margins, shutdown margin with single failure safety reactivity factor and burn-up.

III) The measured and calculated worth values for each control plate have the same profile and slope along the axial extraction range. In addition, there is a very good agreement between the measured and calculated total worth value of different control plates for all core configurations.

IV) For the shutdown margin, the calculated values are slightly less than the measured ones. However, both calculated and measured values are very close. In addition, both measured and calculated shutdown margin values are highly greater than the assigned value as stated in the design criteria (SM ≥ 3000 pcm).

V) The calculated worth value of Cobalt Irradiation Device (CID) is nearly the same as the measured value. This means that the applied calculational model of the cobalt is quite accurate to calculate the cobalt worth.

VI) For the reactor powers below 6 MW, it was noticed that a small variation in the power leads to a large variation in the Xenon equilibrium level. However, for the reactor powers above ~ 6 MW, the variation of Xenon equilibrium level with reactor power becomes less up to about 20 MW where the maximum reactivity becomes considerably constant (~3600 pcm = 4.8 $). This large negative reactivity has to be considered during the fuel management to obtain a reasonable operating cycle

References

[1] Research Reactor Core Conversion from the use of Highly Enriched Uranium to the use of Low Enriched Uranium Fuel Guidebook, IAEA, Vienna (1980).

[2] I. Bhuiyan, M.A.W. Mondal, M.Rahman, M.M. Sarker, M.Q.Huda, M.S. Shadatullah, T.K.Chakroborty, and M.J.H.Khan. “In-core Fuel Management , Safety , and Thermal Hydraulics Studies for Upgrading TRIGA MARK II Research Reactor,” Institute of Nuclear Science & Technology, AERE, Ganakbari, Savar, Bangladesh, IGORR (1999).

[3] H.C. Honeck, “ENDF/B” – Specification for an Evaluated Nuclear Data File for Reactor Application”, Brookhaven National Laboratory Report BNL-50066.

[4] Applications and Results for the Supercell Option of the WIMS-D4M Code, W.L. Wordruff and C.I. Costescu (ANL), International meeting on reduced,

enrichment for researh and test reactors, Paris, France (1994).
[5] K. Andrzejewski and T. Kulikowska, Methods and Codes for Neutronic Calculations of the MARIA Research Reactor, Institute of atomic energy, Poland (1998).
[6] R. Nabbi and J. Wolters, A Sophisticated Computational Method for HEU-LUE Conversion of the German FRJ-2 Research Reactor Using MCNP, Research Center Julich, Germany (1997).
[7] Yoshihiro Nakano, Yoshiro Funayama and Teruo Nakajima, Neutronic Characteristics of JRR-4 LEU Core, Japan Atomic Energy Research Institute, Japan.
[8] G. Hordsy, Cs. Marjucy, A. Simonits, M. Telbisz, Determinstic and Monte Carlo Calculations for the Budapest research Reactor, KFKI Atomic Energy Research Institute Hungary, RETRR. Sao Paulo, Brazil (1998).
[9] DIN/GN/001-96 New isotopes in the WIMS library.
[10] Askew, Fayers & Kemshell, A general description of the lattice code WIMS, UKAEA (1967).
[11] POS_WIMS. MTR_PC User manual. Julio (1993).
[12] CITVAP 3.1. MTR_PC 2.6 User Manual. Julio (1995).
[13] HXS 4.0 MTR_PC 2.6 User manual. Julio (1995).
[14] 0767 5370 3IBLI 001 1O: Operation Manual.
[15] 0767 5370 3IBLI 001 1O. MPR Reactivity Excess Measurement Procedure.

Received August 13, 2003
Accepted November 9, 2003